Inorg. Chem. **2004**, *43*, 342–350

Ab Initio Calculations and Normal Coordinate Analysis of Ruthenium Tris-α-diimine Complexes

Bruce D. Alexander[†] **and Trevor J. Dines***

Division of Physical and Inorganic Chemistry, Carnelley Building, University of Dundee, Dundee, DD1 4HN U.K.

Received June 24, 2003

For the first time, a full scaled quantum chemical normal coordinate analysis has been performed on $[Ru(LL')_3]^{2+}$ complexes, where LL′ = 2,2′-bipyrazine (bpz) or 2,2′-bipyrimidine (bpm). Geometric structures were fully optimized using density functional theory and an effective core potential basis set. The infrared and Raman spectra were calculated using the optimized geometries. The results of the calculations provide a highly satisfactory fit to the experimental infrared and Raman spectra, and the potential energy distributions allow a detailed understanding of the vibrational bands therein.

Introduction

Ruthenium(II) complexes with α-diimine ligands, such as 2,2′-bipyridine (bpy), 2,2′-bipyrazine (bpz), and 2,2′-bipyrimidine (bpm), have been the subject of many detailed investigations owing to their value in photochemistry and photophysics,[1−9] with complexes involving 2,2′-bipyridine being the most extensively studied. The chemical and physical properties of bipyridyl complexes can be tailored to a great extent by variation of the central metal or by introduction of different functionalities onto the bipyridyl ligands, thus offering a remarkable flexibility. Perhaps the most important example of the use of these complexes is as photosensitizers in the new generation of solar cells, i.e., Grätzel cells, where sensitizers such as Ru(2,2′-bipyridyl-4,4′-dicarboxylato)$_2$-*cis*-(NCS)$_2$ are typically chemisorbed onto nanocrystalline titanium dioxide by pendant carboxylic acid groups.

Resonance Raman (RR) and time-resolved resonance Raman (TR^3) spectroscopies have been used to great effect in investigations into the nature of the lowest excited states of ruthenium (II) tris-polypyridyl complexes.[10−12] Initially TR^3 provided the most conclusive evidence of a localized ^{3}MLCT excited state.[11−13] Woodruff and co-workers[11,12] observed bands in the TR^3 spectrum of $[Ru(bpy)_3]^{2+}$ attributed to both the ground-state neutral bpy and radical anion $bpy^{\bullet-}$ ligands thus providing powerful evidence that the ^{3}MLCT state could best be formalized as $[Ru^{III}(bpy)_2(bpy^{\bullet-})]^{2+}$. Despite numerous studies subsequently reporting similar work on related molecules,[10,13−16] the vibrational band assignments remain either based on chemical intuition or by comparison with the normal coordinate analysis of both the ground state, and the ^{3}MLCT state of $[Ru(bpy)_3]^{2+}$ reported by Kincaid and co-workers.[17,18]

However, there are limitations with these methods for assigning infrared and Raman bands in both the ground and

* To whom correspondence should be addressed. E-mail: t.j.dines@dundee.ac.uk. Fax: 44-1382-345517.

† Present address: Département de Chimie Minérale, Analytique et Appliquée, University of Geneva, Sciences II, 30 quai E.-Ansermet, 1211 Geneva, Switzerland. E-mail: bruce.alexander@chiam.unige.ch.

(1) DeArmond, M. K.; Carlin, C. M. *Coord. Chem. Rev.* **1981**, *36*, 325.
(2) DeArmond, M. K.; Myrick, M. L. *Acc. Chem. Res.* **1989**, *22*, 364.
(3) Kalyanasundaram, K. *Coord. Chem. Rev.* **1982**, *46*, 159.
(4) Ross, H. B.; Boldaji, M.; Rillema, D. P.; Blanton, C. B.; White, R. P. *Inorg. Chem.* **1989**, *28*, 1013.
(5) Khan, M. M. T.; Bhardwaj, R. C.; Bhardwaj, C. *Polyhedron* **1990**, *9*, 1243.
(6) Kalyanasundaram, K.; Grätzel, M. *Coord. Chem. Rev.* **1998**, *77*, 347.
(7) Haque, S. A.; Tachibana, Y.; Willis, R. L.; Moser, J.-E.; Grätzel, M.; Klug, D. R.; Durrant, J. R. *J. Phys. Chem. B* **2000**, *104*, 538.
(8) Tachibana, Y.; Haque, S. A.; Mercer, I. P.; Durrant, J. R.; Klug, D. R. *J. Phys. Chem. B* **2000**, *104*, 1198.
(9) Bach, U.; Tachibana, Y.; Moser, J.-E.; Haque, S. A.; Durrant, J. R.; Grätzel, M.; Klug, D. R. *J. Am. Chem. Soc.* **1999**, *121*, 7445.
(10) Gardner, J. S.; Strommen, D. P.; Szulbinski, W. S.; Su, H.; Kincaid, J. R. *J. Phys. Chem. A* **2003**, *107*, 351.
(11) Bradley, P. G.; Kress, N.; Hornberger, B. A.; Dallinger, R. F.; Woodruff, W. H. *J. Am. Chem. Soc.* **1981**, *103*, 7441.
(12) Dallinger, R. F.; Woodruff, W. H. *J. Am. Chem. Soc.* **1979**, *101*, 4391.
(13) Danzer, G. D.; Kincaid, J. R. *J. Phys. Chem.* **1990**, *94*, 3976.
(14) Danzer, G. D.; Kincaid, J. R. *J. Raman Spectrosc.* **1992**, *23*, 681.
(15) Danzer, G. D.; Golus, J. A.; Kincaid, J. R. *J. Am. Chem. Soc.* **1993**, *115*, 8643.
(16) Virdee, H. R.; Hester, R. E. *J. Phys. Chem.* **1984**, *88*, 451.
(17) Strommen, D. P.; Mallick, P. K.; Danzer, G. D.; Lumpkin, R. S.; Kincaid, J. R. *J. Phys. Chem.* **1990**, *94*, 1357.
(18) Mallick, P. K.; Danzer, G. D.; Strommen, D. P.; Kincaid, J. R. *J. Phys. Chem.* **1988**, *92*, 5628.

10.1021/ic034721l CCC: $27.50
Published on Web 12/10/2003

excited states. The reported empirical normal coordinate analysis was, out of necessity, simplified by treating $[Ru(bpy)_3]^{2+}$ as a single bpy ligand coordinated to Ru(II) and considering only in-plane vibrations. Until recently, it was unfeasible to perform quantum chemical calculations on molecules of this size. With the continual development of computational resources, and more importantly, the increasing use of density functional theory (DFT), such calculations are now possible. Indeed, a number of DFT investigations into the molecular structure, the nature of the excited states and the redox behavior of ruthenium tris-polypyridyl complexes have been reported.[19−23] However, as yet, no known scaled quantum mechanical force field (SQM-FF) investigations into ruthenium(II) tris-α-diimine complexes have been reported. We report for the first time a full SQM-FF normal coordinate analysis of two ruthenium tris-α-diimine complexes, which provides a detailed analysis of their vibrational spectra, essential for an understanding of the behavior of these complexes upon adsorption onto surfaces and the properties of excited states.

Experimental Section

Both $[Ru(bpm)_3]Cl_2$ and $[Ru(bpz)_3]Cl_2$ were prepared following literature methods.[24,25] In both cases the complexes were prepared by reflux of the appropriate ligand with $[Ru(DMSO)_4]Cl_2$ in water for 20 h. $[Ru(DMSO)_4]Cl_2$ was prepared following the procedure of Evans, Spencer, and Wilkinson.[26] 2,2′-Bipyrimidine was purchased from a commercial supplier (Aldrich), whereas the 2,2′-bipyrazine had been prepared according to the method of Crutchley and Lever.[25]

Infrared spectra were recorded using 1% (w/w) pressed KBr disks in a Perkin-Elmer 1710x Fourier transform spectrometer with a resolution of 4 cm^{-1}. The FT-IR spectrometer was fitted with a deuterated triglycerine sulfate detector (DTGS) and KBr beam splitter. Resonance Raman (RR) spectra were recorded using a Spex 1403 double monochromator fitted with a Hamamatsu R928 photomultiplier detector. Excitation was provided by Coherent Radiation Innova 90-6 or Spectra-Physics Series 2000 argon ion lasers. Excitation was in the range 457.9−514.5 nm at a maximum power of 100 mW for the 514.5 and 488.0 nm laser lines and 30 mW using the 457.9 nm line. The typical spectral slit width was ca. 4 cm^{-1}. Samples were prepared as crushed powders of ca. 1% ruthenium complex in KBr.

Computational Details

All calculations were performed using the *Gaussian 98* program,[27] at the Hartree−Fock and B3-LYP levels using the 3-21G and LanL2DZ basis sets. However, Hartree−Fock calculations gave poorer geometries and vibrational spectra, due to the neglect of electron correlation, and the results are not reported here. The LanL2DZ basis set is an effective core potential (ECP) basis set which utilizes the Dunning−Huzinaga double-ζ basis functions (DZ) for carbon, nitrogen, and hydrogen atoms,[28] along with the Los Alamos effective core potential for the Ru core electrons with DZ functions for Ru valence orbitals.[29−31] The ground-state structures of both $[Ru(bpm)_3]^{2+}$ and $[Ru(bpz)_3]^{2+}$ were optimized, assuming D_3 symmetry. For computation of IR and Raman spectra and the potential energy distributions associated with the vibrational modes, the Cartesian force constants, dipole derivatives and, when possible, polarizability derivatives obtained from the *Gaussian 98* output were expressed in terms of internal coordinates. Scaling factors were applied to the force constants before input into a normal coordinate analysis program derived from those of Schachtschneider.[32] Normal coordinate analysis was initially performed without scaling. Scaled normal coordinate analysis followed the scaling method of Pulay.[33] At the B3-LYP/LanL2DZ level a scale factor of 0.90 was applied to all force constants involving motion of the hydrogen atoms, and a scale factor of 1.025 was applied to all other force constants in order to yield the best fit to the experimental data.

Both $[Ru(bpm)_3]^{2+}$ and $[Ru(bpz)_3]^{2+}$ contain 55 atoms; thus, there are 159 normal modes, which transform under D_3 symmetry as $\Gamma_{3N-6} = 27a_1 + 26a_2 + 53e$. Modes transforming as a_1 or e are Raman-active, whereas those transforming as a_2 or e are IR-active. Despite optimizing the geometries of both complexes under D_3 symmetry, both HF-SCF and B3-LYP calculations of the normal modes of vibration revealed a small degree of mixing between modes of different symmetry. Thus, both dications were initially treated under C_1 symmetry for the normal coordinate analysis before analysis of the dominant symmetry coordinates in the potential energy distributions (PEDs) enabled facile separation of the normal modes into a_1, a_2, and e symmetry blocks.

Results and Discussion

Ab initio calculations were initially performed on $[Ru(bpm)_3]^{2+}$ and $[Ru(bpz)_3]^{2+}$ at the B3-LYP/3-21G level, although the calculated vibrations were found to require an unrealistic set of scale factors for both complexes, and improvement was found at the B3-LYP/LanL2DZ level. The unscaled and scaled vibrational wavenumbers and the PEDs from the SQM-FF calculations are reported in Tables 1 and 2 for

(19) Daul, C.; Baerends, E. J.; Vernooijs, P. *Inorg. Chem.* **1994**, *33*, 3538.
(20) Stoyanov, S. R.; Villegas, J. M.; Rillema, D. P. *Inorg. Chem.* **2002**, *41*, 2941.
(21) Zheng, K. C.; Wang, J. P.; Peng, W. L.; Liu, X. W.; Yun, F. C. *THEOCHEM* **2002**, *582*, 1.
(22) Monat, J. E.; Rodriguez, J. H.; McCusker, J. K. *J. Phys. Chem. A* **2002**, *106*, 7399.
(23) Zheng, K. C.; Wang, J.; Shen, Y.; Kuang, D.; Yun, F. *J. Phys. Chem. A* **2001**, *105*, 7248.
(24) Hunziker, M.; Ludi, A. *J. Am. Chem. Soc.* **1977**, *99*, 7370.
(25) Crutchley, R. J.; Lever, A. B. P. *Inorg. Chem.* **1982**, *21*, 2276.
(26) Evans, I. P.; Spencer, A.; Wilkinson, G. *J. Chem. Soc., Dalton Trans.* **1973**, 204.
(27) Frisch, M. J.; Trucks, G. W.; Schlegel, H. B.; Scuseria, G. E.; Robb, M. A.; Cheeseman, J. R.; Zakrzewski, V. G.; Montgomery, J. A., Jr.; Stratmann, R. E.; Burant, J. C.; Dapprich, S.; Millam, J. M.; Daniels, A. D.; Kudin, K. N.; Strain, M. C.; Farkas, O.; Tomasi, J.; Barone, V.; Cossi, M.; Cammi, R.; Mennucci, B.; Pomelli, C.; Adamo, C.; Clifford, S.; Ochterski, J.; Petersson, G. A.; Ayala, P. Y.; Cui, Q.; Morokuma, K.; Malick, D. K.; Rabuck, A. D.; Raghavachari, K.; Foresman, J. B.; Cioslowski, J.; Ortiz, J. V.; Stefanov, B. B.; Liu, G.; Liashenko, A.; Piskorz, P.; Komaromi, I.; Gomperts, R.; Martin, R. L.; Fox, D. J.; Keith, T.; Al-Laham, M. A.; Peng, C. Y.; Nanayakkara, A.; Gonzalez, C.; Challacombe, M.; Gill, P. M. W.; Johnson, B. G.; Chen, W.; Wong, M. W.; Andres, J. L.; Head-Gordon, M.; Replogle, E. S.; Pople, J. A. *Gaussian 98*, revision A.5; Gaussian, Inc.: Pittsburgh, PA, 1998.
(28) Dunning, T. H., Jr.; Hay, P. A. In *Modern Theoretical Chemistry*; Schaefer, H. F., III, Ed.; Plenum: New York, 1976; Vol. 3, p 1.
(29) Hay, P. J.; Wadt, W. R. *J. Chem. Phys.* **1985**, *82*, 270.
(30) Hay, P. J.; Wadt, W. R. *J. Chem. Phys.* **1985**, *82*, 299.
(31) Wadt, W. R.; Hay, P. J. *J. Chem. Phys.* **1985**, *82*, 284.
(32) Schachtschneider, J. H. *Vibrational Analysis of Polyatomic Molecules*; Technical Reports 231 and 57; Shell Development Co.: Houston, 1964; Vol. Parts V, VI.
(33) Pulay, P.; Fogarasi, G.; Pongor, G.; Boggs, J. E.; Vargha, A. *J. Am. Chem. Soc.* **1983**, *105*, 7037.

Table 1. Vibrational Spectrum of $[Ru(bpm)_3]^{2+}$ Calculated at the B3-LYP/LanL2DZ Level

mode	$\tilde{\nu}$/cm^{-1} unscaled	$\tilde{\nu}$/cm^{-1} scaled	potential energy distribution (%)
			a_1
ν_1	3273	3106	ν(C2H) (18), ν(C3H) (22), ν(C2H)′ (17), ν(C3H)′ (21)
ν_2	3255	3089	ν(C2H) (29), ν(C3H) (10), ν(C4H) (11), ν(C2H) (23)
ν_3	3244	3079	ν(C3H) (13), ν(C4H) (34), ν(C4H) (16), ν(C4H)′ (21)
ν_4	1601	1605	S_{8b} (66)
ν_5	1554	1549	S_{8a} (63)
ν_6	1498	1496	S_{19a} (16), S_{19b} (16), ν(C6C6′) (31)
ν_7	1437	1386	δ_{ip}(C2H) (18), δ_{ip}(C3H) (14), δ_{ip}(C2H) (14), δ_{ip}(C3H) (11)
ν_8	1370	1348	S_{8b} (13), ν(C6C6′) (11), δ_{ip}(C4H) (35)
ν_9	1308	1280	S_{14} (86)
ν_{10}	1247	1227	S_{8a} (11), S_{19a} (18), δ_{ip}(C2H) (28), δ_{ip}(C4H) (21)
ν_{11}	1122	1104	S_{19a} (33), δ_{ip}(C3H) (45)
ν_{12}	1089	1083	S_1 (12), S_{19b} (38), δ_{ip}(C2H) (11), δ_{ip}(C4H) (11)
ν_{13}	1039	1026	S_1 (37), S_{12} (48)
ν_{14}	1013	975	δ_{op}(C2H) (24), δ_{op}(C3H) (55), δ_{op}(C4H) (37)
ν_{15}	1005	952	δ_{op}(C2H) (56), δ_{op}(C4H) (46)
ν_{16}	865	874	δ_{op}(C6C6′) (37), S_4 (52), Chel.tor-1 (10)
ν_{17}	852	816	δ_{op}(C2H) (22), δ_{op}(C3H) (49), δ_{op}(C4H) (18)
ν_{18}	796	796	S_1 (14), ν(C6C6′) (12), S_{6b} (37), S_{12} (13)
ν_{19}	673	674	S_{6a} (67), S_{6b} (13)
ν_{20}	570	578	δ_{op}(C6C6′) (33), S_4 (46)
ν_{21}	479	486	δ_{ip}(NRuN′) (12), S_{16a} (30), S_{16b} (44), Chel.tor-1 (11)
ν_{22}	374	378	ν(C6C6′) (29), ν(RuN) (10), S_{6a} (18), S_{6b} (13), Chel.def-1 (13)
ν_{23}	290	295	δ_{ip}(NRuN′) (16), δ_{op}(C6C6′) (13), S_{16a} (15), S_{16b} (54)
ν_{24}	246	249	Chel.def-1 (79)
ν_{25}	150	152	ν(RuN) (65), S_{6b} (22)
ν_{26}	120	121	δ_{ip}(NRuN′) (25), S_{16a} (49), Chel.tor-1 (27)
ν_{27}	38	38	δ_{ip}(NRuN′) (46), Chel.tor-1 (49)
			a_2
ν_{28}	3272	3106	ν(C2H) (23), ν(C3H) (32), ν(C2H) (10), ν(C3H) (16)
ν_{29}	3255	3089	ν(C2H) (33), ν(C3H) (12), ν(C4H) (13), ν(C2H)′ (22)
ν_{30}	3244	3078	ν(C3H) (11), ν(C4H) (28), ν(C4H)′ (19), ν(C4H) (20)
ν_{31}	1605	1610	S_{8b} (72)
ν_{32}	1558	1554	S_{8a} (65)
ν_{33}	1464	1428	S_{19a} (30), δ_{ip}(C3H) (10), δ_{ip}(C4H) (27)
ν_{34}	1439	1399	S_{19b} (30), δ_{ip}(C2H) (38), δ_{ip}(C3H) (17)
ν_{35}	1265	1277	S_{14} (10), δ_{ip}(C4H) (24), Chel.def-2 (12), δ_{ip}(C4H) (19)
ν_{36}	1258	1252	S_{14} (55), δ_{ip}(C2H) (15), S_{14} (10)
ν_{37}	1158	1143	S_{19b} (17), δ_{ip}(C2H) (16), S_{12} (26)
ν_{38}	1131	1113	S_{19b} (17), δ_{ip}(C3H) (50)
ν_{39}	1074	1073	S_1 (22), S_{19b} (16), S_{12} (35)
ν_{40}	1038	1010	S_1 (63), S_{12} (28)
ν_{41}	1022	975	δ_{op}(C2H) (25), δ_{op}(C3H) (57), δ_{op}(C4H) (34)
ν_{42}	1006	952	δ_{op}(C2H) (54), δ_{op}(C4H) (49)
ν_{43}	854	832	δ_{op}(C3H) (19), S_4 (63)
ν_{44}	792	786	δ_{op}(C2H) (16), δ_{op}(C3H) (29), δ_{op}(C4H) (13), S_4 (30)
ν_{45}	692	692	S_{6b} (81)
ν_{46}	646	647	S_{6a} (84)
ν_{47}	508	515	S_{19a} (13), Chel.def-2 (39), δ_{ip}(NRuN′) (12), S_{16a} (15)
ν_{48}	471	477	Chel.def-2 (26), S_{16a} (24), S_{16b} (30)
ν_{49}	443	451	δ_{op}(C6C6′) (24), S_4 (10), S_{16a} (25), S_{16b} (41)
ν_{50}	319	323	ν(RuN) (43), δ_{ip}(NRuN′) (23), S_{16b} (10)
ν_{51}	175	178	ν(RuN) (31), δ_{op}(C6C6′) (23), S_{16b} (11), Chel.tor-2 (13)
ν_{52}	87	88	δ_{ip}(NRuN′) (14), δ_{op}(C6C6′) (39), S_{16a} (30)
ν_{53}	51	52	δ_{ip}(NRuN′) (34), Chel.tor-2 (53)
			e
ν_{54}	3272	3106	ν(C2H) (31), ν(C3H) (46)
ν_{55}	3272	3105	ν(C2H) (17), ν(C3H) (23), ν(C2H)′ (21), ν(C3H)′ (28)
ν_{56}	3257	3090	ν(C2H) (23), ν(C3H) (10), ν(C2H)′ (22), ν(C3H)′ (10)
ν_{57}	3255	3089	ν(C2H) (48), ν(C3H) (16), ν(C4H) (17)
ν_{58}	3244	3078	ν(C4H) (21), ν(C3H) (18), ν(C4H) (49)
ν_{59}	3244	3078	ν(C3H) (10), ν(C4H) (27), ν(C3H) (15), ν(C4H) (42)
ν_{60}	1608	1612	S_{8b} (72)
ν_{61}	1600	1604	S_{8b} (67)
ν_{62}	1557	1553	S_{8a} (65)
ν_{63}	1554	1547	S_{8a} (64)
ν_{64}	1496	1495	S_{19a} (16), S_{19b} (15), ν(C6C6′) (32), S_{12} (10)
ν_{65}	1463	1428	S_{19a} (30), δ_{ip}(C3H) (11), δ_{ip}(C4H) (27)
ν_{66}	1440	1403	S_{19b} (31), δ_{ip}(C2H) (38), δ_{ip}(C3H) (15)
ν_{67}	1439	1386	δ_{ip}(C2H) (14), δ_{ip}(C3H) (11), δ_{ip}(C2H) (18), δ_{ip}(C3H) (14)
ν_{68}	1369	1346	S_{8b} (13), ν(C6C6′) (11), δ_{ip}(C4H) (35)
ν_{69}	1307	1279	S_{14} (82)

Table 1 (Continued)

mode	$\tilde{\nu}$/cm^{-1} unscaled	$\tilde{\nu}$/cm^{-1} scaled	potential energy distribution (%)
			e
ν_{70}	1266	1278	δ_{ip}(C4H) (20), S_{14} (11), δ_{ip}(C4H) (23), Chel.def-2 (12)
ν_{71}	1253	1250	S_{14} (10), S_{14} (53), δ_{ip}(C2H) (15)
ν_{72}	1246	1221	S_{8a} (11), S_{19a} (18), δ_{ip}(C2H) (27), δ_{ip}(C3H) (10), δ_{ip}(C4H) (21)
ν_{73}	1157	1141	S_{19b} (16), δ_{ip}(C2H) (17), S_{12} (29)
ν_{74}	1132	1115	S_{19b} (14), δ_{ip}(C3H) (51)
ν_{75}	1119	1101	S_{19a} (38), δ_{ip}(C3H) (42)
ν_{76}	1088	1081	S_1 (12), S_{19b} (41), δ_{ip}(C2H) (10), δ_{ip}(C4H) (10)
ν_{77}	1076	1075	S_1 (23), S_{19b} (19), S_{12} (29)
ν_{78}	1038	1017	S_1 (32), S_{12} (44)
ν_{79}	1038	1012	S_1 (53), S_{12} (26)
ν_{80}	1012	974	δ_{op}(C3H) (13), δ_{op}(C4H) (10), δ_{op}(C2H)′ (16), δ_{op}(C3H)′ (43), δ_{op}(C4H)′ (29)
ν_{81}	1006	974	δ_{op}(C2H) (14), δ_{op}(C3H) (42), δ_{op}(C4H) (31), δ_{op}(C3H)′ (14)
ν_{82}	1004	949	δ_{op}(C2H) (57), δ_{op}(C4H) (42)
ν_{83}	1002	949	δ_{op}(C2H) (57), δ_{op}(C4H) (45)
ν_{84}	863	872	δ_{op}(C6C6′) (36), S_4 (52), Chel.tor-1 (10)
ν_{85}	855	833	δ_{op}(C3H) (16), S_4 (68)
ν_{86}	849	813	δ_{op}(C2H) (24), δ_{op}(C3H) (48), δ_{op}(C4H) (17)
ν_{87}	793	792	S_1 (15), ν(C6C6′) (11), S_{6b} (34), S_{12} (10)
ν_{88}	791	785	δ_{op}(C2H) (17), δ_{op}(C3H) (29), δ_{op}(C4H) (13), S_4 (26)
ν_{89}	694	694	S_{6b} (82)
ν_{90}	668	670	S_{6a} (67), S_{6b} (15)
ν_{91}	647	649	S_{6a} (85)
ν_{92}	568	575	δ_{op}(C6C6′) (32), S_4 (44), S_{16a} (11)
ν_{93}	505	512	S_{19a} (10), Chel.def-2 (38), S_{16a} (15), S_{16b} (11)
ν_{94}	490	497	Chel.def-2 (21), S_{16a} (22)
ν_{95}	458	465	S_{16a} (21), S_{16b} (45)
ν_{96}	439	447	δ_{op}(C6C6′) (21), S_{16a} (20), S_{16b} (54)
ν_{97}	368	372	ν(C6C6′) (30), S_{6a} (17), S_{6b} (16), Chel.def-1 (15)
ν_{98}	335	339	ν(RuN) (26), Chel.def-1 (41)
ν_{99}	279	283	δ_{op}(C6C6′) (15), S_{16a} (21), S_{16b} (47), δ_{ip}(NRuN′) (12)
ν_{100}	223	225	Chel.def-1 (32), δ_{ip}(NRuN′)′ (11), ν(RuN)′ (11)
ν_{101}	196	198	ν(RuN) (48), δ_{op}(C6C6′) (16)
ν_{102}	175	177	ν(RuN) (44), S_{6b} (17), ν(RuN)′ (15)
ν_{103}	112	113	S_{16a} (39), Chel.tor-1 (35), δ_{ip}(NRuN′) (11)
ν_{104}	80	81	δ_{ip}(NRuN′) (11), δ_{op}(C6C6′) (50), S_{16a} (32)
ν_{105}	40	40	δ_{ip}(NRuN′) (16), Chel.tor-1′ (35), δ_{ip}(NRuN′)′ (22)
ν_{106}	32	32	Chel.tor-2 (10), δ_{ip}(NRuN′) (13), δ_{ip}(NRuN′)′ (13), Chel.tor-2 (58)

$[Ru(bpm)_3]^{2+}$ and $[Ru(bpz)_3]^{2+}$, respectively, and the atom numbering schemes are shown in Figure 1. Wilson coordinates are used to describe the vibrations of the aromatic rings.[34,35] Symmetry coordinates specific to deformations and torsions of the five-membered chelate ring, as defined by Pulay,[36] are labeled Chel.def-1 and Chel.def-2 and Chel.tor-1 and Chel.tor-2, respectively. These are shown in Figure 2. Construction of symmetry coordinates, in accordance with D_3 symmetry, followed the general format

$$a_1 \quad (i_1 + i_2) + (j_1 + j_2) + (k_1 + k_2)$$

$$a_2 \quad (i_1 - i_2) + (j_1 - j_2) + (k_1 - k_2)$$

e

$$2(i_1 \pm i_2) - (j_1 \pm j_2) - (k_1 \pm k_2) \text{ and } (j_1 \pm j_2) - (k_1 \pm k_2)$$

where i, j, and k refer to the three ligands, and the subscripts 1 and 2 refer to the diazine rings on either side of these, which are related by C_2 symmetry. For internal coordinates which appear only once in each ligand, e.g., r(C6C6′) and chelate ring coordinates, the symmetry coordinates were of the form $(i + j + k)$, etc. This system was chosen in order to give the tidiest possible potential energy distributions. In Tables 1 and 2, the deformation coordinate δ(NRuN′) refers to two nitrogen atoms from different ligands, and the designation prime (′) after a coordinate refers to the second contribution of an e-type degenerate pair, i.e., of the form $(j_1 \pm j_2) - (k_1 \pm k_2)$ given above.

The results of the scaled calculations at the B3-LYP/LanL2DZ level are compared with the infrared spectra (Figure 3) in Table 3 and RR spectra (Figure 4) in Tables 4 and 5. The predicted ν(CH) modes span a relatively narrow range, and in contrast to $[Ru(bpz)_3]^{2+}$, these modes are subject to a considerable degree of mixing for $[Ru(bpm)_3]^{2+}$. It can be seen from the PEDs that only a small degree of mixing between symmetry coordinates of different symmetry classes exists despite the apparently poor description of symmetry by the calculations; i.e., a_1 modes are separated from a_2 modes and e modes. This problem predominantly occurs for the ν(CH) modes with e symmetry, i.e., ν_1 of $[Ru(bpm)_3]^{2+}$ is heavily mixed but predominantly of a_1 symmetry with a small degree of mixing with modes of e symmetry. There were no instances of mixing between a_1 and a_2 symmetry coordinates.

(34) Varsanyi, G. *Vibrational Spectra of Benzene Derivatives*; Academic Press: New York, 1969; Vol. 25.
(35) Wilson, E. B. *Phys. Rev.* **1934**, *45*, 706.
(36) Pulay, P.; Fogarasi, G.; Pang, F.; Boggs, J. E. *J. Am. Chem. Soc.* **1979**, *101*, 2550.

Table 2. Vibrational Spectrum of $[Ru(bpz)_3]^{2+}$ Calculated at the B3-LYP/LanL2DZ Level

mode	$\tilde{\nu}$/cm^{-1} unscaled	$\tilde{\nu}$/cm^{-1} scaled	potential energy distribution (%)
			a_1
ν_1	3278	3111	ν(C2H) (41), ν(C2H) (11), ν(C2H)′ (36)
ν_2	3276	3109	ν(C2H) (46), ν(C2H) (15), ν(C2H)′ (26)
ν_3	3244	3078	ν(C3H) (48), ν(C5H) (19), ν(C3H) (16)
ν_4	1595	1593	S_{8b} (53), ν(C6C6′) (15), δ_{ip}(C5H) (10)
ν_5	1536	1543	S_{8a} (80)
ν_6	1508	1490	S_{8b} (14), S_{19b} (22), ν(C6C6′) (21), δ_{ip}(C2H) (16)
ν_7	1432	1388	S_{19a} (19), δ_{ip}(C2H) (16), δ_{ip}(C3H) (40)
ν_8	1372	1329	ν(C6C6′) (14), δ_{ip}(C5H) (59)
ν_9	1300	1270	S_{8b} (17), S_{19a} (10), δ_{ip}(C2H) (38), δ_{ip}(C5H) (13)
ν_{10}	1249	1263	S_{14} (93)
ν_{11}	1182	1170	S_{19a} (35), S_{19b} (15), δ_{ip}(C3H) (29), S_{12} (10)
ν_{12}	1079	1079	S_1 (48), S_{12} (14)
ν_{13}	1053	1054	S_{19b} (39), δ_{ip}(C2H) (11), S_{12} (38)
ν_{14}	1006	947	δ_{op}(C2H) (44), δ_{op}(C3H) (61)
ν_{15}	969	917	δ_{op}(C6C6′) (10), δ_{op}(C2H) (10), δ_{op}(C5H) (60), δ_{op}(C5H)′ (17)
ν_{16}	890	855	δ_{op}(C6C6′) (14), δ_{op}(C2H) (39), δ_{op}(C3H) (30), S_4 (16)
ν_{17}	806	804	S_{6a} (15), δ_{op}(C5H) (11), S_4 (22)
ν_{18}	800	800	S_{6a} (15), δ_{op}(C5H) (11), S_4 (25)
ν_{19}	670	672	ν(RuN) (12), S_{6a} (43), S_{6b} (32)
ν_{20}	595	604	δ_{op}(C6C6′) (30), S_4 (36), S_{16a} (21), Chel.tor-1 (31)
ν_{21}	482	488	δ_{ip}(NRuN′) (11), δ_{op}(C6C6′) (23), S_{16a} (28), S_{16b} (30)
ν_{22}	375	378	S_1 (13), ν(C6C6′) (26), ν(RuN) (11), S_{6a} (15), S_{6b} (11), Chel-def-1 (17)
ν_{23}	267	271	Chel.def-1 (30), S_{16b} (52)
ν_{24}	250	253	Chel.def-1 (50), S_{16b} (21)
ν_{25}	149	150	ν(RuN) (63), S_{6b} (25)
ν_{26}	127	129	δ_{ip}(NRuN′) (27), S_{16a} (45), Chel.tor-1 (26)
ν_{27}	37	37	δ_{ip}(NRuN′) (45), δ_{op}(C6C6′) (10), Chel.tor-1 (45)
			a_2
ν_{28}	3276	3109	ν(C2H) (61), ν(C2H)′ (22)
ν_{29}	3245	3079	ν(C2H) (11), ν(C3H) (81)
ν_{30}	3235	3070	ν(C5H) (64), ν(C5H) (32)
ν_{31}	1588	1590	S_{8b} (68)
ν_{32}	1547	1559	S_{8a} (73)
ν_{33}	1477	1429	S_{19b} (28), δ_{ip}(C2H) (22), δ_{ip}(C3H) (17), δ_{ip}(C5H) (25)
ν_{34}	1435	1399	S_{19a} (39), δ_{ip}(C3H) (28)
ν_{35}	1352	1303	δ_{ip}(C2H) (27), δ_{ip}(C5H) (33)
ν_{36}	1232	1242	S_{14} (81)
ν_{37}	1198	1179	S_{19a} (22), δ_{ip}(C3H) (35)
ν_{38}	1124	1113	S_{19b} (27), δ_{ip}(C2H) (18), S_{12} (29)
ν_{39}	1042	1045	S_1 (12), S_{19b} (19), S_{12} (35)
ν_{40}	1017	1026	S_1 (76), S_{12} (14)
ν_{41}	1007	948	δ_{op}(C2H) (42), δ_{op}(C3H) (64)
ν_{42}	972	919	δ_{op}(C2H) (20), δ_{op}(C5H) (82)
ν_{43}	876	829	δ_{op}(C2H) (46), δ_{op}(C3H) (42), δ_{op}(C5H) (13)
ν_{44}	785	797	S_4 (97)
ν_{45}	707	705	S_{6a} (66), S_{6b} (21)
ν_{46}	636	639	ν(RuN) (12), S_{6a} (22), S_{6b} (58)
ν_{47}	524	531	δ_{ip}(NRuN′) (12), S_{16a} (56), Chel.tor-2 (16)
ν_{48}	472	477	S_{19a} (15), Chel.def-2 (56), S_{16a} (10)
ν_{49}	396	403	δ_{op}(C6C6′) (34), S_{16b} (58)
ν_{50}	322	326	ν(RuN) (43), δ_{ip}(NRuN′) (24), S_{16b} (11)
ν_{51}	175	177	ν(RuN) (22), δ_{op}(C6C6′) (13), Chel.tor-2 (10), ν(RuN)′ (16)
ν_{52}	92	94	δ_{op}(C6C6′) (41), S_{16a} (25), S_{16b} (11)
ν_{53}	56	56	δ_{ip}(NRuN′) (40), Chel.tor-2 (47)
			e
ν_{54}	3278	3111	ν(C2H) (27), ν(C2H)′ (48), ν(C2H) (14)
ν_{55}	3276	3109	ν(C2H) (62), ν(C2H)′ (26)
ν_{56}	3248	3082	ν(C5H) (33), ν(C3H) (11), ν(C5H) (42)
ν_{57}	3245	3080	ν(C2H) (11), ν(C3H) (82)
ν_{58}	3244	3078	ν(C3H) (17), ν(C3H) (52), ν(C5H) (18)
ν_{59}	3236	3070	ν(C5H) (32), ν(C5H) (64)
ν_{60}	1593	1592	S_{8b} (57)
ν_{61}	1590	1591	S_{8b} (43), ν(C6C6′) (12), S_{8b}′ (13)
ν_{62}	1546	1558	S_{8a} (74)
ν_{63}	1536	1542	S_{8a} (79)
ν_{64}	1506	1488	S_{8b} (14), S_{19b} (20), ν(C6C6′) (21), δ_{ip}(C2H) (17)
ν_{65}	1481	1433	S_{19b} (28), δ_{ip}(C2H) (21), δ_{ip}(C3H) (17), δ_{ip}(C5H) (24)
ν_{66}	1435	1398	S_{19a} (39), δ_{ip}(C3H) (28)
ν_{67}	1433	1388	S_{19a} (19), δ_{ip}(C2H) (16), δ_{ip}(C3H) (40)
ν_{68}	1372	1330	ν(C6C6′) (14), δ_{ip}(C5H) (59)

Table 2 (Continued)

mode	$\tilde{\nu}$/cm^{-1} unscaled	$\tilde{\nu}$/cm^{-1} scaled	potential energy distribution (%)
			e
ν_{69}	1350	1302	δ_{ip}(C2H) (26), δ_{ip}(C5H) (33)
ν_{70}	1295	1266	S_{8b} (14), S_{14} (16), δ_{ip}(C2H) (32), δ_{ip}(C5H) (12)
ν_{71}	1249	1262	S_{14} (77)
ν_{72}	1230	1240	S_{14} (80)
ν_{73}	1198	1179	S_{19a} (22), δ_{ip}(C3H) (35)
ν_{74}	1181	1169	S_{19a} (35), S_{19b} (15), δ_{ip}(C3H) (29), S_{12} (11)
ν_{75}	1122	1110	S_{19b} (25), δ_{ip}(C2H) (19), S_{12} (30)
ν_{76}	1077	1075	S_1 (43), S_{19a} (11), S_{19b} (15), δ_{ip}(C2H) (14)
ν_{77}	1044	1047	S_1 (27), S_{19b} (15), S_{12} (24)
ν_{78}	1039	1043	S_{19b} (28), S_{12} (41)
ν_{79}	1021	1030	S_1 (64), S_{12} (19)
ν_{80}	1004	946	δ_{op}(C2H) (35), δ_{op}(C3H) (67)
ν_{81}	1004	945	δ_{op}(C2H) (39), δ_{op}(C3H) (65)
ν_{82}	963	916	δ_{op}(C5H)′ (55), δ_{op}(C5H) (23)
ν_{83}	962	916	δ_{op}(C6C6′) (12), δ_{op}(C2H) (12), δ_{op}(C5H) (71)
ν_{84}	884	849	δ_{op}(C6C6′) (15), δ_{op}(C2H) (43), δ_{op}(C3H) (26), S_4 (15)
ν_{85}	872	826	δ_{op}(C2H) (50), δ_{op}(C3H) (40), δ_{op}(C5H) (11)
ν_{86}	802	802	S_1 (11), S_{6a} (19), S_4′ (25)
ν_{87}	801	801	S_4′ (14), S_4 (42)
ν_{88}	783	796	δ_{op}(C5H) (14), S_4 (32), S_4′ (31)
ν_{89}	706	704	S_{6a} (67), S_{6b} (21)
ν_{90}	661	663	ν(RuN) (11), S_{6a} (43), S_{6b} (33)
ν_{91}	641	644	ν(RuN) (12), S_{6a} (21), S_{6b} (59)
ν_{92}	594	603	δ_{op}(C6C6′) (31), S_4 (34), S_{16a} (22), Chel.tor-1 (13)
ν_{93}	529	537	S_{16a} (60), Chel.tor-2 (17)
ν_{94}	483	489	S_{19a} (12), Chel.def-2 (41)
ν_{95}	460	466	δ_{op}(C6C6′) (14), S_{16a} (23), S_{16b} (28), Chel.def-2′ (18)
ν_{96}	394	401	δ_{op}(C6C6′) (29), S_{16b} (61)
ν_{97}	369	373	S_1 (10), ν(C6C6′) (26), S_{6a} (12), S_{6b} (14), Chel.def-1 (24)
ν_{98}	336	340	ν(RuN) (29), Chel.def-1 (37)
ν_{99}	255	259	δ_{op}(C6C6′) (10), S_{16a} (10), S_{16b} (66), δ_{ip}(NRuN′) (10)
ν_{100}	226	229	Chel.def-1 (29), δ_{ip}(NRuN′)′ (11), ν(RuN)′ (13)
ν_{101}	194	196	ν(RuN) (45), δ_{op}(C6C6′) (14), S_{16b} (10)
ν_{102}	174	176	ν(RuN) (43), S_{6b} (19), ν(RuN)′ (14)
ν_{103}	120	121	S_{16a} (36), Chel.tor-1 (33), δ_{ip}(NRuN′) (11)
ν_{104}	85	86	δ_{op}(C6C6′) (52), S_{16a} (25)
ν_{105}	41	41	δ_{ip}(NRuN′) (25), Chel.tor-1′ (25), δ_{ip}(NRuN′)′ (11), Chel.tor-2 (18)
ν_{106}	36	36	Chel.tor-1′ (14), δ_{ip}(NRuN′)′ (23), Chel.tor-2 (41)

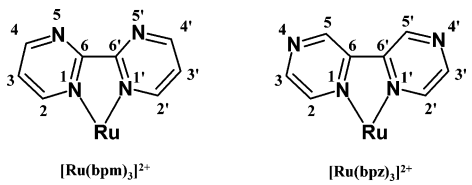

Figure 1. Atom numbering scheme used for $[Ru(bpm)_3]^{2+}$ and $[Ru(bpz)_3]^{2+}$ complexes.

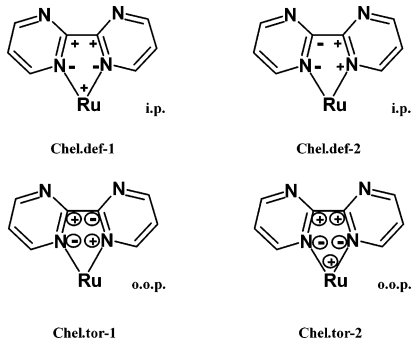

Figure 2. Definition of five-membered chelate ring torsions and deformations.

For $[Ru(bpm)_3]^{2+}$ and $[Ru(bpz)_3]^{2+}$, the fit of the calculated vibrations to the infrared and RR spectra is highly satisfactory (Tables 3−5). In all cases the strong bands in the infrared and RR spectra are predicted with good agreement, although such agreement was not found for the scaled B3-LYP/3-21G spectra. The strongest bands in the infrared spectra of both complexes are assigned to vibrations involving the 8a, 8b, 19a, and 19b (CC and CN stretches) and δ_{op}(C3H) coordinates. Furthermore, from Table 3 it can be seen that modes of e symmetry are the strongest bands and that, as expected, no a_1 modes are present in the infrared spectra of either complex.

As stated previously, not only do the results of the ab initio calculations presented in Tables 1 and 2 represent the first treatment of ions such as $[Ru(bpm)_3]^{2+}$ or $[Ru(bpz)_3]^{2+}$ as a whole, but they are also the first accurate SQM-FF normal coordinate analysis of this class of molecules. Comparison of the PEDs listed in Tables 1 and 2 with literature normal coordinate analysis of bpm or bpz ligands is difficult as the descriptions of the normal modes have either been reported pictorially, in terms of vector diagrams with corresponding Cartesian atomic displacements, or as kinetic energy distributions, KEDs. As Neto et al. have indicated, a comparison of KEDs and PEDs is not strictly valid.[37] Neto et al. used the 328 cm^{-1} (a_g) mode of bpz as an example to highlight the differences between the KEDs and PEDs. The force constant

(37) Neto, N.; Muniz-Miranda, M.; Sbrana, G. *Spectrochim. Acta, Part A* **1994**, *50*, 357.

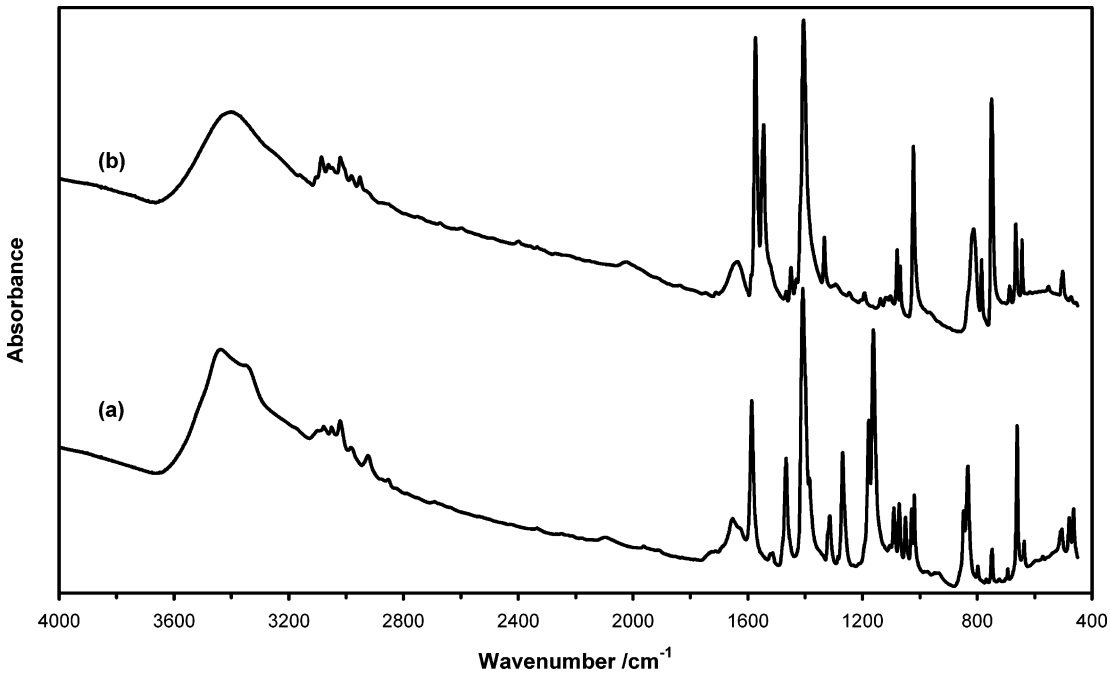

Figure 3. Infrared spectra of (a) $[Ru(bpz)_3]^{2+}$ and (b) $[Ru(bpm)_3]^{2+}$.

for C6C6′ stretching was reported to have a predominant role in the PED but was negligible in the KED of the 328 cm^{-1} mode. However, Cartesian displacements revealed that this mode was described by one pyrazine ring translating with respect to the other, i.e., inter-ring stretching. Furthermore, the corresponding mode in $[Ru(bpz)_3]^{2+}$ is the ν_{22} (a_1) mode, observed at 378 cm^{-1}. The PED given in Table 2 reveals that the ν(C6C6′) symmetry coordinate has a large contribution to the normal mode but is mixed with several other symmetry coordinates. It is unusual to report KEDs, and Neto et al. represent the only known KED for normal modes reported in the literature.

Where PEDs have been used for this class of molecule,[17,18,38] normal modes have tended to be described in terms of individual bond stretching, angle deformation, etc. For example, Strommen et al. report ν_{10}, calculated for $[Ru(bpy)_3]^{2+}$ at 1272 cm^{-1}, to consist of 38% $\nu(C_2N)$, 36% $\nu(C_2C_3)$, 20% $\nu(C_6N)$, 12% $\nu(C_4C_5)$, and 11% $\delta_{ip}(C_3C_4)$.[17] Thus, a band observed at 1276 cm^{-1} has been assigned to the ν_{10} mode by Strommen et al. throughout the literature.[15,39,40] By using Wilson coordinates, a more detailed description of the normal modes is achieved. The corresponding mode to the ν_{10} mode of Strommen et al. is ν_9 for $[Ru(bpm)_3]^{2+}$, predicted at 1280 cm^{-1}. Table 1 shows that this mode is clearly dominated by the S_{14} coordinate with negligible contributions from other symmetry coordinates. Thus, the PEDs shown in Tables 1 and 2 represent a significantly clearer description of the normal modes of vibration of $[Ru(bpm)_3]^{2+}$ and $[Ru(bpz)_3]^{2+}$ that might otherwise not have been possible.

Although the empirical force field normal coordinate analysis of Strommen et al. resulted in a satisfactory comparison between calculated and experimental data,[17] this came from the treatment of $[Ru(bpy)_3]^{2+}$ as an 21-atom unit, i.e., the hypothetical $[Ru(bpy)]^{2+}$ species. Thus, no information regarding symmetry was available, nor was there any information regarding polarizability derivatives, and hence Raman intensities. Furthermore, Strommen et al. only considered in-plane modes. All of these are available through the ab initio calculations in the present case. Calculated Raman intensities are of limited value at the HF-SCF level due to limitations in the description of polarizability derivatives. Although these can be calculated using the B3-LYP method, this can only be done using the lengthy numerical integration procedure. This was not considered to be justified in the present case because the Raman spectra reported in Figure 4 are recorded under resonance conditions. Polarizability derivatives obtained from B3-LYP/LanL2DZ calculation are not then valid as they take no account of resonance enhancement. Nevertheless, both the Raman intensities and the description of symmetry provided by the present model, which are absent in the metal−ligand model of Strommen et al., provide valuable information which can help prevent incorrect band assignments. For example, the pair of intense bands at 1484 and 1514 cm^{-1} in the RR spectra of $[Ru(bpz)_3]^{2+}$ (Table 5) might have been assigned to the ν_{64} (e) ν(C6C6′)/S_{19b} and ν_6 (a_1) S_{19b}/ν(C6C6′) modes, respectively, based purely on the band positions. However, no depolarized bands are observed in this region of the spectrum for $[Ru(bpz)_3]^{2+}$. No modes of e symmetry are observed for ions of this nature as the Herzberg−Teller RR mechanism is generally thought to be negligible.[41,42] Modes of e symmetry may be allowed through Jahn−Teller activity in

(38) Ould-Moussa, L.; Castella-Ventura, M.; Kassab, E.; Poizat, O.; Strommen, D. P.; Kincaid, J. R. *J. Raman Spectrosc.* **2000**, *31*, 377.
(39) Edmiston, M. J.; Peacock, R. D. *Spectrochim. Acta, Part A* **1996**, *52*, 191.
(40) Srnova-Sloufova, I.; Vlckova, B.; Snoeck, T. L.; Stufkens, D. J.; Matejka, P. *Inorg. Chem.* **2000**, *39*, 3551.
(41) Clark, R. J. H.; Turtle, P. C.; Strommen, D. P.; Streusand, B.; Kincaid, J. R.; Nakamoto, K. *Inorg. Chem.* **1977**, *16*, 84.

Table 3. Infrared Band Wavenumber Positions (cm^{-1}) for $[Ru(bpm)_3]^{2+}$ and $[Ru(bpz)_3]^{2+}$

$[Ru(bpm)_3]^{2+}$			$[Ru(bpz)_3]^{2+}$			assignment		$[Ru(bpm)_3]^{2+}$			$[Ru(bpz)_3]^{2+}$			assignment	
$\tilde{\nu}$(obs)	int	$\tilde{\nu}$(calc)[a]	$\tilde{\nu}$(obs)	int	$\tilde{\nu}$(calc)[a]			$\tilde{\nu}$(obs)	int	$\tilde{\nu}$(calc)[a]	$\tilde{\nu}$(obs)	int	$\tilde{\nu}$(calc)[a]		
3159	vw		3176	vw							1162	vs	1169	ν_{94} (e)	S_{19a}, δ_{ip}(C3H)
3105	vw	3106				ν_{55} (e)	ν(C3H)	1138	w	1143				ν_{37} (a_2)	S_{12}, S_{19b}, δ_{ip}(C2H)
			3099	w	3082	ν_{56} (e)	ν(C5H)				1125	sh	1113	ν_{38} (a_2)	S_{12}, S_{19b}
3086	m	3089				ν_{57} (e)	ν(C2H)	1118	w	1113				ν_{38} (a_2)	δ_{ip}(C3H)
			3078	m	3080	ν_{29} (a_2)	ν(C3H)				1104	vw	1110	ν_{75} (e)	S_{12}, S_{19b}
3061	w	3078				ν_{58} (e)	ν(C4H)	1103	w	1101				ν_{75} (e)	δ_{ip}(C3H), S_{19a}
			3051	m	3070	ν_{59} (e)	ν(C5H)				1090	m	1110		
3047	vw	3078				ν_{59} (e)	ν(C4H)	1079	m	1082				ν_{76} (e)	S_{19b}
3020	m		3021	m							1072	m	1075	ν_{76} (e)	S_1
3007	vw							1068	m	1075				ν_{77} (e)	S_{12}
2981	w		2981	w							1050	m	1043	ν_{78} (e)	S_{12}
2952	w		2923	vw							1029	m	1030	ν_{79} (e)	S_1
			2851	vw				1022	s	1017				ν_{78} (e)	S_{12}
2399	vw										1019	m	1026	ν_{40} (a_2)	S_1
			2099	w				984	vvw	975	976	w		ν_{41} (a_2)	δ_{op}(C3H), δ_{op}(C4H)
2023	vw							967	vw	974	948	w		ν_{81} (e)	δ_{op}(C3H), δ_{op}(C4H)
			1652	m							932	w			
1588	vw	1605									848	m	829	ν_{43} (a_2)	δ_{op}(C2H), δ_{op}(C3H)
			1586	vs	1590	ν_{31} (a_2)	S_{8b}	832	sh	833				ν_{85} (e)	S_4
1573	vs	1604				ν_{61} (e)	S_{8b}				833	s	827	ν_{85} (e)	δ_{op}(C2H), δ_{op}(C3H)
1545	s	1548	1555	w	1542	ν_{63} (e)	S_{8a}	813	m	832				ν_{43} (a_2)	S_4
1520	sh		1520	w	1490	ν_{64} (e)	ν(C6C6′), S_{19b}				798	w	800	ν_{87} (e)	δ_{op}(C3H), S_4
			1513	w				785	m	786				ν_{44} (a_2)	δ_{op}(C3H), S_4
			1477	sh							768	w			
1466	w		1466	s	1433	ν_{65} (e)	S_{19b}, δ_{ip}(C5H)	750	vs	785	748	m		ν_{88} (e)	δ_{op}(C3H), S_4
1449	m	1428				ν_{33} (a_2)	S_{19a}, δ_{ip}(C4H)				722	w	705	ν_{45} (a_2)	S_{6a}
1430	w	1428				ν_{65} (e)	S_{19a}, δ_{ip}(C4H)				700	vw			
			1408	vs	1399	ν_{34} (a_2)	S_{19a}				694	w	704	ν_{89} (e)	S_{6a}
1406	vs	1399				ν_{34} (a_2)	δ_{ip}(C2H), S_{19b}	688	w	692				ν_{45} (a_2)	S_{6b}
1374	sh	1386	1385	s	1388	ν_{67} (e)	δ_{ip}(C2H), δ_{ip}(C3H)	666	m	670	661	s	663	ν_{90} (e)	S_{6a}
			1349	sh	1329	ν_{68} (e)	δ_{ip}(C5H)	644	m	670				ν_{91} (e)	S_{6a}
1333	m	1347				ν_{68} (e)	δ_{ip}(C4H)				641	vw	644	ν_{91} (e)	S_{6b}
			1314	m	1303	ν_{35} (a_2)	δ_{ip}(C5H), δ_{ip}(C2H)	618	vvw		636	w	639	ν_{46} (a_2)	S_{6b}
1294	w	1279				ν_{69} (e)	S_{14}				595	w	603	ν_{92} (e)	S_4, δ_{op}(C6C6′)
			1285	w	1266	ν_{70} (e)	δ_{ip}(C2H)	552	w		571	w			
			1269	s	1242	ν_{36} (a_2)	S_{14}				505	w	489	ν_{94} (e)	Chel.def-2
1246	w	1252				ν_{71} (e)	S_{14}	502	m	515				ν_{47} (a_2)	Chel.def-2
			1231	vw	1240	ν_{72} (e)	S_{14}	473	w	477	480	m	477	ν_{48} (a_2)	S_{16b}, S_{16a}, Chel.def-2
1193	w		1192	sh	1179						464	m	466	ν_{95} (e)	S_{16b}, S_{16a}
			1178	s	1169	ν_{73} (e)	δ_{ip}(C3H)								

[a] From scaled calculated values at the B3-LYP/LanL2DZ level.

the degenerate excited state, although the lack of depolarized bands and analysis of the Raman intensities reveals that the ν_{64} mode is predicted to be very weak and an intense band is predicted at 1543 cm^{-1}, corresponding to the $\nu_5(a_1)$ mode. Thus, the correct assignments for these bands are the ν_6 (a_1) S_{19b}/ν(C6C6′) mode for the 1484 cm^{-1} band and the ν_5 (a_1) S_{8a} mode for the 1514 cm^{-1} band. These assignments are also consistent with those given for $[Ru(bpm)_3]^{2+}$ in Table 4.

Finally, the use of ab initio calculations that treat the whole $[Ru(LL')_3]^{2+}$ cation may be useful in determining the symmetry, and thus the delocalization of charge, in the ^{3}MLCT excited state. Calculations of the ^{3}MLCT excited-state geometry and vibrational spectrum, using the CIS or CASSCF methods, should provide a clear idea of the rearrangement of charge in the ^{3}MLCT excited state, with respect to the $^1A_1$ ground state. Nevertheless, this may prove difficult as Daul et al. have already shown that mixing occurs between the singlet and triplet MLCT excited states of $[Ru(bpy)_3]^{2+}$.[19] Clearly the use of a basis set larger than that used here would be critical for such work, not only to better describe the molecular symmetry, but also to better describe the excited states, although only a very limited range of basis sets is available for second row transition metals. In particular, the addition of polarization functions might be essential. Furthermore, modeling of the vibrational spectrum of the ^{3}MLCT excited state should reveal any symmetry lowering through the appearance of imaginary frequencies. This would determine whether the vibrations of the excited state appear at a distinct set of values, as suggested for the delocalized case, or a mixture of vibrations attributed to bpy and $bpy^{\bullet-}$ as suggested by Bradley et al. for the localized case.[11]

Conclusions

Ab initio calculations were performed at the B3-LYP/LanL2DZ level for the $[Ru(bpm)_3]^{2+}$ and $[Ru(bpz)_3]^{2+}$ cations. These calculations, and the resultant normal coor-

(42) Dines, T. J.; Peacock, R. D. *J. Chem. Soc., Faraday Trans. 1* **1988**, *84*, 3445.

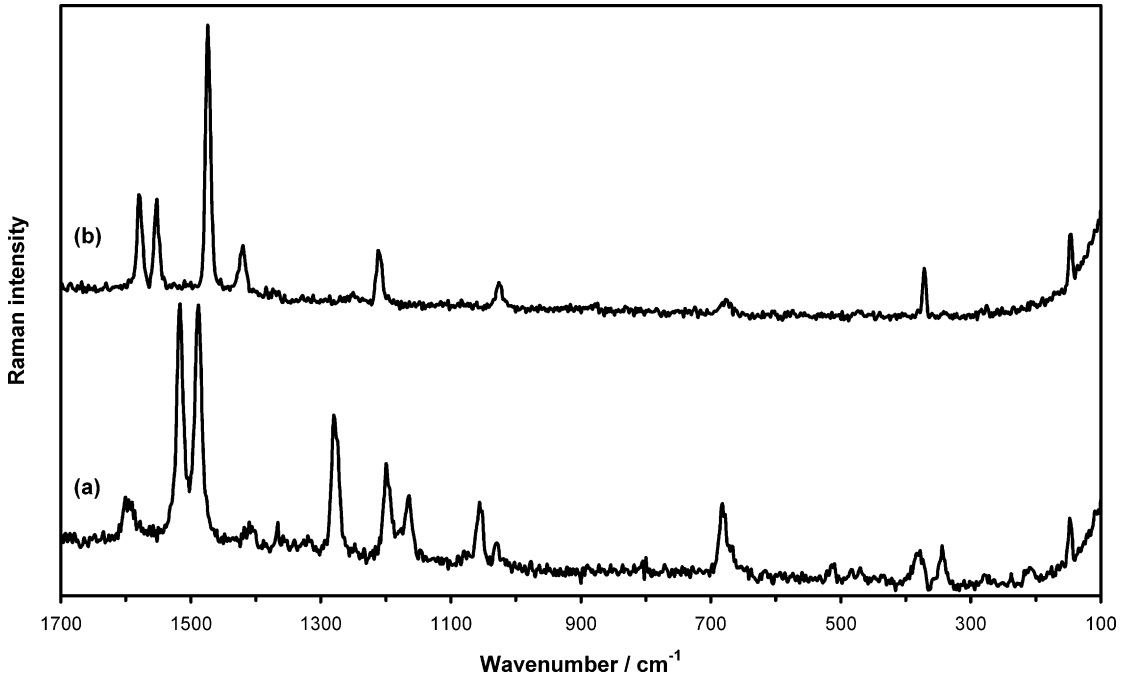

Figure 4. Resonance Raman spectra of (a) $[Ru(bpz)_3]^{2+}$ and (b) $[Ru(bpm)_3]^{2+}$ recorded with 457.9 nm excitation.

Table 4. Resonance Raman Band Wavenumber Positions and Relative Intensities (Normalized with Respect to the 1472 cm^{-1} Band) for $[Ru(bpm)_3]^{2+}$, Excited at 457.9 nm

$\tilde{\nu}$(obs)/cm^{-1}	rel int	$\tilde{\nu}$(calc)[a]/cm^{-1}	assignment	
1580	24	1604	ν_4 (a_1)	S_{8b}
1552	42	1549	ν_5 (a_1)	S_{8a}
1544	9	1547	ν_{63} (e)	S_{8a}
1500	3			
1484	13	1495	ν_{64} (e)	ν(C6C6′)
1472	100	1496	ν_6 (a_1)	ν(C6C6′)
1421	14	1428	ν_{65} (e)	S_{19a}, δ_{ip}(C4H)
1336	12	1348	ν_8 (a_1)	δ_{ip}(C4H)
1245	4	1250	ν_{71} (e)	S_{14}
1212	17	1221	ν_{72} (e)	δ_{ip}(C2H), δ_{ip}(C4H)
1203	30	1227	ν_{10} (a_1)	δ_{ip}(C2H), δ_{ip}(C4H)
862	7	874	ν_{16} (a_1)	S_4, δ_{op}(C6C6′)
788	9	796	ν_{18} (a_1)	S_{6b}
677	12	674	ν_{19} (a_1)	S_{6a}
475	18	486	ν_{21} (a_1)	S_{16b}, S_{16a}
466	5	465	ν_{95} (e)	S_{16b}
379	1	378	ν_{22} (a_1)	ν(C6C6′)
315	10	295	ν_{23} (a_1)	S_{16b}
291	31	285		
281	11	283	ν_{99} (e)	S_{16b}
267	5	249	ν_{24} (a_1)	Chel.def-1
120	62	121	ν_{26} (a_1)	S_{16a}, Chel.tor-1

[a] From scaled calculated values at the B3-LYP/LanL2DZ level.

Table 5. Resonance Raman Band Wavenumber Positions and Relative Intensities (Normalized with Respect to the 1484 cm^{-1} Band) for $[Ru(bpz)_3]^{2+}$, Excited at 457.9 nm

$\tilde{\nu}$(obs)/cm^{-1}	rel int	$\tilde{\nu}$(calc)[a]/cm^{-1}	assignments	
1598	36	1593	ν_4 (a_1)	S_{8b}
1514	96	1543	ν_5 (a_1)	S_{8a}
1484	100	1490	ν_6 (a_1)	S_{19b}, ν(C6C6′)
1409	15	1398	ν_{66} (e)	S_{19a}
1397	1	1388	ν_7 (a_1)	δ_{ip}(C3H)
1350	83	1329	ν_8 (a_1)	δ_{ip}(C5H)
1275	86	1263	ν_{10} (a_1)	S_{14}
1193	41	1179	ν_{73} (e)	δ_{ip}(C3H), S_{19a}
1163	29	1170	ν_{11} (a_1)	S_{19a}, δ_{ip}(C3H)
1075	2	1079	ν_{12} (a_1)	S_1
1051	36	1047	ν_{77} (e)	S_1, S_{12}
1029	9	1030	ν_{79} (e)	S_1
980	3			
803	3	802	ν_{86} (e)	S_4, S_{6a}
779	4	797	ν_{18} (a_1)	S_4
681	44	672	ν_{19} (a_1)	S_{6a}, S_{6b}
666	7	664	ν_{90} (e)	S_{6a}, S_{6b}
651	3	644	ν_{91} (e)	S_{6b}
508	11	488	ν_{21} (a_1)	S_{16b}, S_{16a}, δ_{op}(C6C6′)
480	4	489	ν_{94} (e)	S_{6a}
463	5	466	ν_{95} (e)	S_{16b}, S_{16a}
381	37	378	ν_{22} (a_1)	ν(C6C6′), Chel.def-1
341	25	340	ν_{98} (e)	Chel.def-1, ν(RuN)
275	10	271	ν_{23} (a_1)	S_{16b}
234	3	253	ν_{24} (a_1)	Chel.def-1
206	11	196	ν_{101} (e)	ν(RuN)

[a] From scaled calculated values at the B3-LYP/LanL2DZ level.

dinate analysis, represent the first full SQM-FF normal coordinate analysis of any ruthenium(II) tris-α-diimine complexes, including all $3N - 6$ modes. Despite poor representation of the molecular symmetry at the B3-LYP/LanL2DZ level, the vibrational modes could be separated into a_1, a_2, or e symmetry classifications from the result of the normal coordinate analysis. Thus, it was possible to accurately fully assign bands in the infrared and Raman spectra for the first time in terms of detailed mode descriptions and symmetry species. Use of Wilson notation provided a description of the symmetry coordinates responsible for certain modes with clarity that was hitherto unattainable. A satisfactory fit to the experimental data was provided by the B3-LYP/LanL2DZ method.

Acknowledgment. One of us (B.D.A.) would like to thank the University of Dundee for a University Scholarship.

IC034721L